Chemical Science

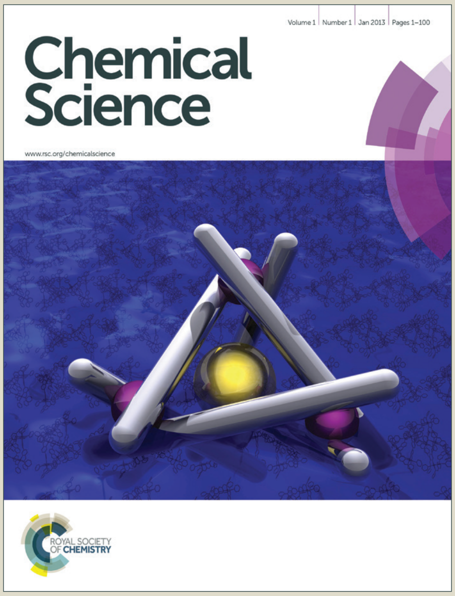

Volume 1 | Number 1 | Jan 2013 | Pages 1–100

Chemical Science

www.rsc.org/chemicalscience

ROYAL SOCIETY OF CHEMISTRY

ROYAL SOCIETY OF CHEMISTRY

www.rsc.org/chemicalscience

Chemical Science RSCPublishing

ARTICLE

Self-assembling 1D core/shell microrods by the introduction of additives: a one-pot and shell-tunable method

Cite this: DOI: 10.1039/x0xx00000x

Received 00th January 2012,
Accepted 00th January 2012

DOI: 10.1039/x0xx00000x

www.rsc.org/

Jun Xu, Hongde Yu, Liulin Yang, Guanglu Wu, Zhiqiang Wang, Dong Wang and Xi Zhang*

Herein, we have developed a one-pot method for the fabrication of one-dimensional core/shell microrods with tunable shell compositions by the introduction of additives. Crystalline dimethyl melamine hydrochloride was utilized as the core, while melamine derivatives with different functional groups, such as pyrene, thiophene and naphthalene diimide, served as additives to regulate the core morphology and adsorbed as the shell. The length and width of such one-dimensional structures can be tuned by varying the molar ratio of core and shell molecules as well as their total concentration. Through X-ray diffraction, the detailed molecular arrangements within the core of microrods were revealed, and the selective effect of additives on specific crystal faces was evaluated. It is anticipated that this work may provide a facile approach for the fabrication of one-dimensional functional materials.

Introduction

One-dimensional (1D) micro/nanostructures are suitable for the transport of electrons, photons and excitons because of the size confinement effect[1-8]. Therefore, they have attracted tremendous attention due to their abundant applications in the fabrication of electronic, photonic and optoelectronic micro/nano devices[9-14]. Recently, increasing efforts have been made to fabricate 1D micro/nanostructures with multi-components and novel topologies (segmented, core/shell or branched) to achieve more complex functionalities[15-23]. 1D micro/nanomaterials with core/shell structures have shown potential applications in various fields such as transistors[24, 25], solar cells[26-28], gas sensing[29, 30], photocatalysis[31], lithium-ion batteries[32] and so forth[33-35]. Leiber et al have synthesized core/shell nanowires with versatile shell compositions by chemical vapor deposition on the nanowire surface, which can be applied for the preparation of coaxially gated nanowire field-effect transistors[24]. Yao and Zhao et al have prepared core/sheath nanowire optical waveguides with a co-precipitation method, which can be used for rapid and sensitive optical detection of gaseous hydrogen peroxide[29]. However, despite of these successful examples, it is still a big challenge to fabricate 1D core/shell structures with tunable shell compositions in a convenient approach.

Herein, we have developed a convenient additive-adsorption method for the fabrication of 1D core/shell microrods with tunable shell compositions. Crystalline dimethyl melamine hydrochloride (Mela-DM•HCl) was applied as the core, while various melaminium derivatives (Mela-M-R, R=Pym, Pm, 2Nm, 3Tm, NDI4, shown in Scheme 1) were utilized as additives to regulate the core morphology and adsorbed as the shell. Simply mixing Mela-DM with Mela-M-R in dichloromethane (DCM) and adding equimolar amount of hydrochloric acid (HCl) led to the formation of self-assembled 1D core/shell microrods with required shell compositions. X-ray diffraction (XRD) was performed to elucidate the possible effect of additives on inducing the 1D morphology.

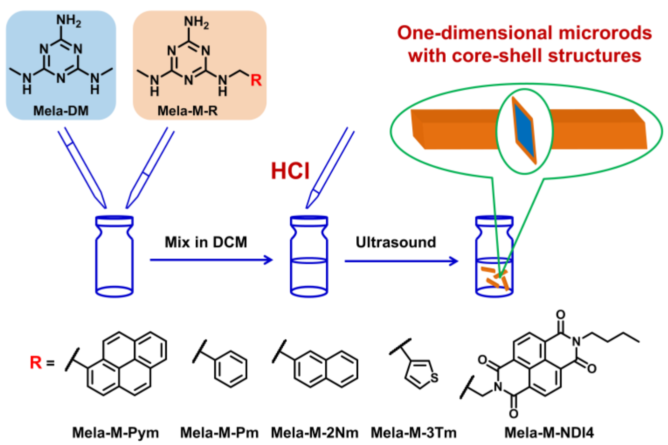

Scheme 1. Fabrication of 1D microrods with core/shell structures in a one-pot approach. The core of microrods is constituted by Mela-DM•HCl, while the shell is formed from Mela-M-R (R=Pym, Pm, 2Nm, 3Tm, NDI4) bearing various functional groups.

Results and discussion

Self-assembled structures of Mela-DM•HCl

The self-assembly of Mela-DM with HCl in DCM leads to the formation of micrometer-sized quadrangular prisms (Figure S1). Such microstructures have rhombus-shaped bases with vertex angles of 50^{o}. Single crystal XRD was employed to reveal the molecular arrangements of Mela-DM•HCl. As shown in Figure 1, protonated Mela-DM molecules are connected by chloride ions to form ribbons, one ribbon further stacks with four adjacent ribbons in the perpendicular direction to produce a 3D network. The driving forces are combined intermolecular interactions, including chloride ion mediated hydrogen bonding and electrostatic interaction in one direction, π-π stacking and hydrogen bonding in the other two directions. Based on the above results, the exposed crystal faces in Mela-DM•HCl microstructures can be determined to be (0,1,0), (1,0,1) and (1,0,-1), and the rhombus-shaped bases correspond to (0,1,0) face (Figure S1b). It should be noted that (1,0,1) and (1,0,-1) faces are identical. Therefore, if the growth perpendicular to (1,0,1) face can be supressed by the introduction of additives, 1D structures could be obtained; otherwise, two-dimensional (2D) assemblies would be acquired.

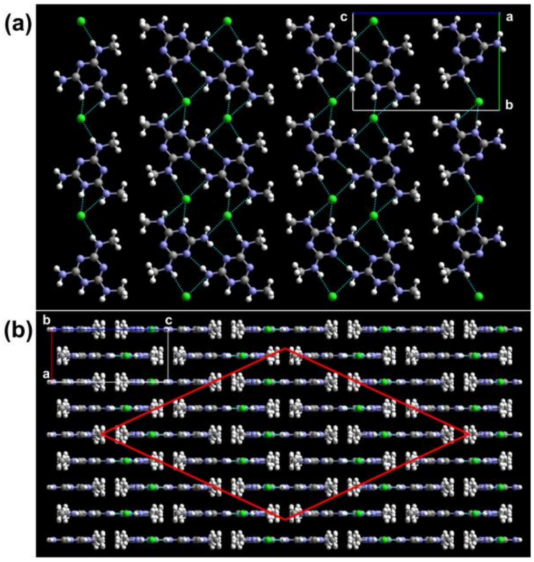

Figure 1. The crystal structures of Mela-DM•HCl (grey: C; white: H; blue: N; green: Cl). The driving forces are chloride ion bridging and hydrogen bonding (a) as well as π-π stacking (b). The red edges of the rhombus (b) indicate the crystal faces of (1,0,1) and (1,0,-1).

Fabrication of 1D core/shell microrods

In a typical preparation, 4.5 mL of Mela-DM solution (1.0 mM in DCM) was mixed with 0.5 mL of Mela-M-R (R=Pym, Pm, 2Nm, 3Tm, NDI4) solution (1.0 mM in DCM) to get a two-component solution with 10% of Mela-M-R, then 1.4 µL of HCl (3.5 M in H_2O) was added. After sonication for 1 min and standing for several hours at room temperature, the solution became turbid, indicating the formation of assemblies with large size. Generally, the suspension should be kept for at least three days to ensure that equilibrium was reached. Assemblies with different molar ratio of Mela-M-R (5, 20%) and in different concentrations (0.5, 2.0 mM) were prepared in similar procedures.

The self-assembly of Mela-DM/Mela-M-Pym(10%)•HCl (1 mM) results in the formation of 1D microrods. As indicated by scanning electron microscopy (SEM) in Figure 2a and 2b, the length of the 1D assemblies is tens of micrometers, while the width is about several hundred nanometers, which is quite uniform. Moreover, side-view SEM reveals that the microrods have rhombus-shaped cross sections with vertex angles of about 50^{o} (Figure 2c), which probably correspond to the (0,1,0) crystal face. Therefore, the growth perpendicular to (0,1,0) face might have been relatively enhanced because of the introduction of additives. Furthermore, fluorescence microscopy image in Figure 2d shows that the microrods emit strong blue fluorescence when excited by UV light (330-385 nm), while confocal fluorescence microscopy image in Figure S2 shows that the periphery of the microrod exhibits much stronger fluorescence than its middle, indicating the formation of core/shell microrods with fluorescent Mela-M-Pym as the shell. The fluorescence spectrum of the microrods was recorded in Figure S3, the peaks in 380, 399 and 422 nm represent the emission of monomer, while the broad peak around 450 nm corresponds to the aggregated state of pyrene.

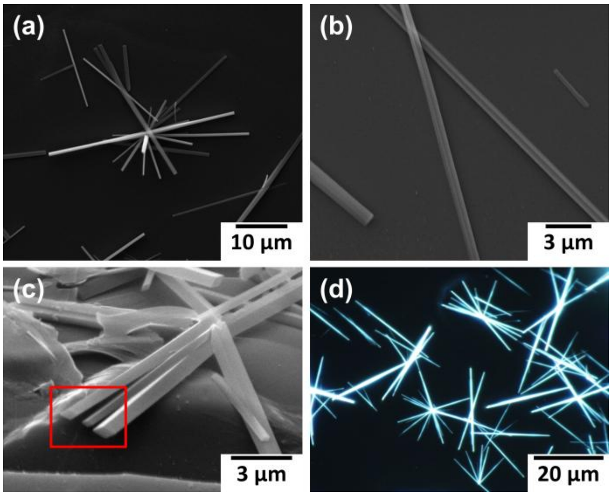

Figure 2. (a,b) SEM images of the microrods formed by Mela-DM/Mela-M-Pym(10%)•HCl (1 mM). (c) Side-view SEM image showing the rhombus-shaped cross sections of the microrods. (d) Fluorescence microscopy image of the microrods.

The length and width of the 1D microrods can be tuned by varying the molar ratio of Mela-DM/Mela-M-Pym and their total concentration. As shown in Figure 3a-c, increasing the molar ratio of Mela-M-Pym from 5% to 10% will narrow the width and increase the length of the 1D microrods, but further increasing the molar ratio to 20% will not cause much change in the morphology of the 1D structures. In Figure 3c, we can also observe the appearance of fluorescent dots formed by Mela-M-Pym•HCl (SEM and fluorescence microscopy images shown in Figure S4), which means further increasing the molar ratio of Mela-M-Pym will lead to the assembly of Mela-M-Pym with HCl instead of co-assembly with Mela-DM•HCl, thus having little effects on the morphology change of the 1D microrods. Moreover, lowing the total concentration of melamine moiety from 2.0 mM to 0.5 mM will lengthen the 1D microrods from about 10 micrometers to over 50 micrometers (Figure 3d-f).

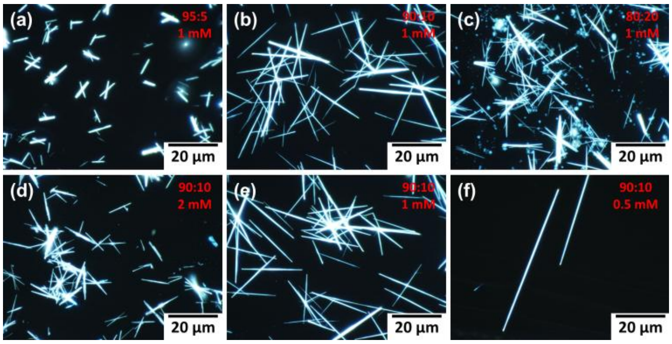

Figure 3. Fluorescence microscopy images of (a) Mela-DM/Mela-M-Pym(5%)•HCl (1 mM); (b) Mela-DM/Mela-M-Pym(10%)•HCl (1 mM); (c) Mela-DM/Mela-M-Pym(20%)•HCl (1 mM); (d) Mela-DM/Mela-M-Pym(10%)•HCl (2 mM); (e) Mela-DM/Mela-M-Pym(10%)•HCl (1 mM); (f) Mela-DM/Mela-M-Pym(10%)•HCl (0.5 mM). All the samples were excited by UV light (330-385 nm).

Growth mechanism of 1D core/shell microrods

In order to investigate the growth mechanism of the 1D core/shell microrods, powder XRD was performed for the unground samples of Mela-DM•HCl microstructures and Mela-DM/Mela-M-Pym(10%)•HCl microrods to reveal the molecular arrangements. As shown in Figure 4, the diffraction peaks in the XRD pattern of Mela-DM/Mela-M-Pym(10%)•HCl microrods were almost the same with Mela-DM•HCl, except for the difference of their intensity. This means Mela-DM•HCl in the microrods is in a crystalline state, with the same molecular arrangements shown in Figure 1. Nevertheless, compared with Mela-DM•HCl microstructures, the peak intensity of (0,1,0) face in Mela-DM/Mela-M-Pym(10%)•HCl microrods decreased dramatically, while the intensity of (0,0,2), (1,0,1) and (2,0,0) faces relatively increased. This result indicates that, for crystalline Mela-DM•HCl within the microrods, the growth perpendicular to (0,1,0) face is relatively strengthened, which is consistent with the SEM observation (Figure 2c). This may be caused by the introduction of Mela-M-Pym additives, which have similar structure with Mela-DM and may interact with specific faces of crystalline Mela-DM•HCl, and then change the growth rates of (0,1,0) and (1,0,1) faces, resulting in the elongation of Mela-DM•HCl microstructures to form 1D microrods. The additives will adsorb on the microrods to form core/shell structures, in which the crystalline Mela-DM•HCl is the core portion, and adsorbed Mela-M-Pym is the shell portion. It should be noted that the microrods would be shortened in length and broadened in width when prepared at -20 °C (Figure S5), which supported that such 1D structures should be the kinetically controlled products.

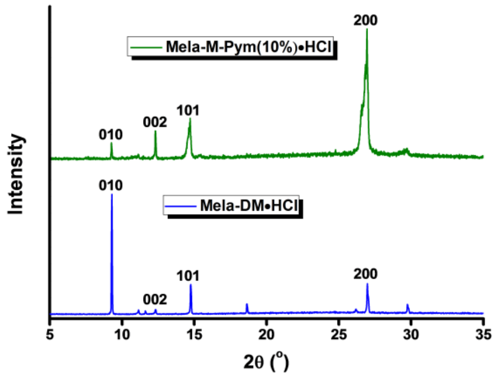

Figure 4. Powder XRD spectra of Mela-DM•HCl (bottom) and Mela-DM/Mela-M-Pym(10%)•HCl (top).

As the additives may alter the growth kinetics of different crystal faces and induce the formation of 1D microrods, in order to clarify the selective effect of additives on (0,1,0) and (1,0,1) faces, it is necessary to investigate the growth mechanisms of the aforementioned faces. Based on different interface structures, the crystal growth mechanisms have been classified mainly into two modes: continuous growth mechanism and 2D nucleation growth mechanism[36, 37]. The Mela-DM•HCl crystal exhibits a chloride ion mediated and hydrogen bonded ribbon in the direction perpendicular to the (0,1,0) face, while the (1,0,1) face is almost parallel to the ribbon. Therefore, abundant hydrogen bonding sites are exposed on (0,1,0) face (Figure S6a), which are suitable for the direct inclusion of Mela-DM into the crystal lattice, thus the growth mechanism may be continuous growth. Whereas, since only methyl groups are exposed (Figure S6b), the (1,0,1) face may grow through a 2D nucleation mechanism in which the formation of a stable crystalline nucleus on the surface is the rate-determining step. This is analogous to the paradigmatic case of urea[38]. Since Mela-M-Pym shares remarkable structural similarity with Mela-DM, it may compete for the adsorption sites and affect the growth of (0,1,0) face. Meanwhile, Mela-M-Pym may adsorb on the (1,0,1) face and inhibit the nucleation process due to the sterical hindrance effect of pyrene, which is fatal to the growth of (1,0,1) face. The additives might have greater inhibition effect on the growth of (1,0,1) face than (0,1,0) face. As a result, the (1,0,1) face will grow slower than the (0,1,0) face when Mela-DM•HCl crystal is exposed to Mela-M-Pym, resulting in the formation of 1D structures.

As the appended pyrene groups may be responsible for the supressed growth on (1,0,1) face, it is anticipated that additives with different substituent groups could also be used for the fabrication of 1D structures. To answer this question, the substituents to Mela-M-R were varied from pyrene to benzene, naphthalene, thiophene and naphthalene diimide. As indicated by SEM in Figure S7, self-assembly of Mela-DM/Mela-M-R (R=Pm, 2Nm, 3Tm, NDI4) led to the formation of 1D microrods in the presence of HCl. It is noticed that, additives with benzene, naphthalene and thiophene groups would induce the formation of 1D micrords with smaller length/width ratio compared with pyrene (Table S1), because these small substituents may bear relatively weak sterical hindrance effect. Such results can further demonstrate that the formation of 1D structures is due to the supressed growth of (1,0,1) face caused by the sterical hindrance of additives. Therefore, this method can be expanded for the preparation of 1D core/shell microrods with diverse shell molecules.

Tuning the fluorescence of Mela-DM/Mela-M-Pym(10%)•HCl

Given that HCl was incorporated into the Mela-DM/Mela-M-Pym(10%)•HCl microrods, the fluorescence of absorbed pyrene groups might be tuned by treating with ammonia gas. As shown in Figure 5a, after exposure to ammonia for merely 20 s, the emission of pyrene monomer increased greatly and the fluorescence of aggregated state decreased, while the morphology of the microrods was almost unchanged (Figure S8). This may be explained as follows: ammonia could permeate into the shell of microrods and interact with HCl, the resulting products may stay in the shell portion and prevent the stacking of pyrene chromophores. As the exposure time may not be enough for ammonia to get into the core portion, the structure of the microrods was still intact.

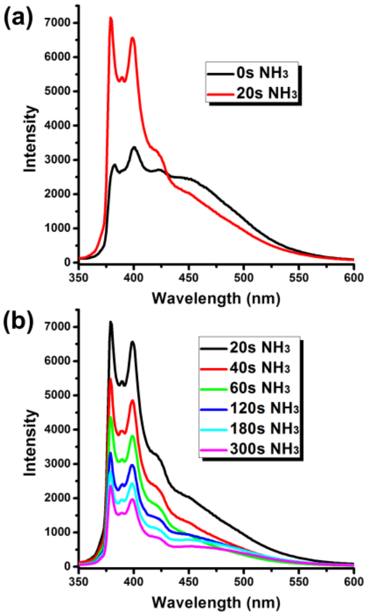

Figure 5. (a) Fluorescence spectra of Mela-DM/Mela-M-Pym(10%)•HCl before and after exposure to ammonia for 20 s. (b) Fluorescence spectra of Mela-DM/Mela-M-Pym(10%)•HCl with increased exposure time to ammonia.

Interestingly, increasing the exposure time to ammonia will lead to the attenuation of the fluorescence intensity. As shown in Figure 5b, when the exposure time was increased from 20 s to 300 s, the fluorescence of the sample decreased significantly. Meanwhile, fluorescence microscopy and SEM images indicated that the structure of the microrods was gradually disrupted (Figure S9). As a stronger base than melamine, ammonia could permeate into the microrods and bind with HCl, which broke the interaction of chloride ion bridging and caused the decomposition of the microrods. In this process, the pyrene moieties in the shell might be buried into the core, thus resulting in a decrease of the fluorescence.

Conclusions

In conclusion, we have successfully prepared 1D core/shell microrods with crystalline Mela-DM•HCl as the core and various Mela-M-R as the shell in a convenient additive-adsorption approach. The length and width of such 1D structures can be tuned by varying the the molar ratio of Mela-DM/Mela-M-Pym and their total concentration. Furthermore, the selective effect of additives on the growth of specific crystal faces is evaluated, giving rise to a possible growth mechanism of the 1D structures. It is expected that various functional groups can be attached to the additive molecules, thus providing a facile approach to fabricate 1D core/shell structures with potential applications in areas such as organic field-effect transistors and organic photonic materials.

Acknowledgements

This work was financially supported by the Foundation for Innovative Research Groups of the National Natural Science Foundation of China (21121004), the National Basic Research Program of China (2013CB834502). The authors thank Prof. Kaibei Yu and Prof. Ruji Wang for single crystal XRD data collection and structure determination. We also thank Mr. Yu Yi for his help in drawing the TOC picture.

Notes and references

MOE Key Lab of Organic Optoelectronics & Molecular Engineering, Department of Chemistry, Tsinghua University, Beijing 100084, P. R. China.

† Electronic Supplementary Information (ESI) available: SEM images of Mela-DM•HCl; confocal fluorescence microscopy image and fluorescence spectrum of Mela-DM/Mela-M-Pym•HCl microrods; SEM and fluorescence microscopy images of Mela-M-Pym•HCl; SEM image of Mela-DM/Mela-M-Pym•HCl microrods prepared at -20 °C; SEM images of Mela-DM/Mela-M-R•HCl microrods; fluorescence microscopy and SEM images of Mela-DM/Mela-M-Pym•HCl after exposure to ammonia; experimental details and compound characterization; details of the single crystal structure of Mela-DM•HCl (CCDC: 1063152). See DOI: 10.1039/b000000x/

1. J. P. Hill, W. Jin, A. Kosaka, T. Fukushima, H. Ichihara, T. Shimomura, K. Ito, T. Hashizume, N. Ishii and T. Aida, Science, 2004, 304, 1481.
2. L. C. Palmer and S. I. Stupp, Acc. Chem. Res., 2008, 41, 1674.
3. L. Zang, Y. Che and J. S. Moore, Acc. Chem. Res., 2008, 41, 1596.
4. Y. Zhao, H. Fu, A. Peng, Y. Ma, D. Xiao and J. Yao, Adv. Mater., 2008, 20, 2859.
5. C. Wang, Y. Guo, Y. Wang, H. Xu, R. Wang and X. Zhang, Angew. Chem. Int. Ed., 2009, 48, 8962.
6. H. Liang, S. Liu and S. Yu, Adv. Mater., 2010, 22, 3925.
7. L. Tian, R. Szilluweit, R. Marty, L. Bertschi, M. Zerson, E. Spitzner, R. Magerle and H. Frauenrath, Chem. Sci., 2012, 3, 1512.

8. N. P. Dasgupta, J. Sun, C. Liu, S. Brittman, S. C. Andrews, J. Lim, H. Gao, R. Yan and P. Yang, Adv. Mater., 2014, 26, 2137.
9. J. Kong, N. R. Franklin, C. Zhou, M. G. Chapline, S. Peng, K. J. Cho and H. Dai, Science, 2000, 287, 622.
10. Y. Huang, X. Duan, Q. Wei and C. M. Lieber, Science, 2001, 291, 630.
11. J. Zhao, J. I. Wong, C. Wang, J. Gao, V. Z. Ng, H. Y. Yang, S. C. Loo and Q. Zhang, Chem. Asian J., 2013, 8, 665.
12. Q. Cui, Y. Zhao and J. Yao, Chem. Sci., 2014, 5, 52.
13. B. Weng, S. Liu, Z. Tang and Y. Xu, RSC Adv., 2014, 4, 12685.
14. Y. Ma, M. Xue, J. Shi and Y. Tan, Nanoscale, 2014, 6, 6828.
15. S. J. Hurst, E. K. Payne, L. Qin and C. A. Mirkin, Angew. Chem. Int. Ed., 2006, 45, 2672.
16. A. J. Mieszawska, R. Jalilian, G. U. Sumanasekera and F. P. Zamborini, Small, 2007, 3, 722.
17. X. Wang and C. S. Ozkan, Nano Lett., 2008, 8, 398.
18. Y. Ner, J. G. Grote, J. A. Stuart and G. A. Sotzing, Angew. Chem. Int. Ed., 2009, 48, 5134.
19. C. Meng, Y. Xiao, P. Wang, L. Zhang, Y. Liu and L. Tong, Adv. Mater., 2011, 23, 3770.
20. Q. Cui, L. Jiang, C. Zhang, Y. Zhao, W. Hu and J. Yao, Adv. Mater., 2012, 24, 2332.
21. Q. Wen, J. Di, Y. Zhao, Y. Wang, L. Jiang and J. Yu, Chem. Sci., 2013, 4, 4378.
22. Y. Zhang, L. Zhang, R. Deng, J. Tian, Y. Zong, D. Jin and X. Liu, J. Am. Chem. Soc., 2014, 136, 4893.
23. J. Zhang, C. Wang, W. Chen, J. Wu and Q. Zhang, RSC Adv., 2015, 5, 25550.
24. L. J. Lauhon, M. S. Gudiksen, D. Wang and C. M. Lieber, Nature, 2002, 420, 57.
25. D. C. Dillen, K. Kim, E. S. Liu and E. Tutuc, Nat. Nanotechnol., 2014, 9, 116.
26. A. L. Briseno, T. W. Holcombe, A. I. Boukai, E. C. Garnett, S. W. Shelton, J. J. Frechet and P. Yang, Nano Lett., 2010, 10, 334.
27. J. Tang, Z. Huo, S. Brittman, H. Gao and P. Yang, Nat. Nanotechnol., 2011, 6, 568.
28. Y. Shi, L. Tan, L. Chen and Y. Chen, Macromolecules, 2014, 47, 1757.
29. J. Zheng, Y. Yan, X. Wang, W. Shi, H. Ma, Y. Zhao and J. Yao, Adv. Mater., 2012, 24, OP194.
30. S. J. Park, O. S. Kwon and J. Jang, Chem. Commun., 2013, 49, 4673.
31. X. Peng, A. C. Santulli, E. Sutter and S. S. Wong, Chem. Sci., 2012, 3, 1262.
32. B. S. Lee, H. S. Yang, H. Jung, S. Y. Jeon, C. Jung, S. W. Kim, J. Bae, C. L. Choong, J. Im, U. I. Chung, J. J. Park and W. R. Yu, Nanoscale, 2014, 6, 5989.
33. Z. Deng, S. Pal, A. Samanta, H. Yan and Y. Liu, Chem. Sci., 2013, 4, 2234.
34. J. S. Bykova, M. D. Lima, C. S. Haines, D. Tolly, M. B. Salamon, R. H. Baughman and A. A. Zakhidov, Adv. Mater., 2014, 26, 7510.
35. M. Mashkour, T. Kimura, F. Kimura, M. Mashkour and M. Tajvidi, RSC Adv., 2014, 4, 52542.
36. G. Dhanaraj, K. Byrappa, V. Prasad and M. Dudley, Springer handbook of crystal growth, Springer: New York, 2010.
37. I. Sunagawa, Crystals: growth, morphology and perfection, Cambridge University Press: Cambridge, 2005.
38. The exposed crystal faces of urea are (0,0,1) and (1,1,0). In the direction perpendicular to (0,0,1) face, urea molecules are connected by strong hydrogen bonding to form infinite chains, while (1,1,0) face is parallel to the hydrogen bonded chains. Therefore, the growth mechanism of (0,0,1) face is continuous growth since the exposed hydrogen bonds are oriented in the growth direction to offer binding sites for urea molecules, whereas (1,0,1) face grows following a birth and spread mechanism since urea molecules can not directly incorporate into the lattice for lack of strong interactions. Such results were demonstrated by molecular dynamics simulations. See: M. Salvalaglio, T. Vetter, F. Giberti, M. Mazzotti and M. Parrinello, J. Am. Chem. Soc., 2012, 134, 17221.